**Electronic Supplementary Information for**

# Effects of trace Si impurities in water on the growth of calcite nanoparticles

*Yuki Kezuka,*[*a] *Hidenobu Murata,*[*b] *Maya Yoshida,*[a] *Kenichiro Eguchi,*[a] *Atsushi Nakahira,*[b,c] *and Masahiko Tajika*[a]

[a.] Shiraishi Central Laboratories Co. Ltd., 4–78, Motohama-cho, Amagasaki, Hyogo 660–0085, Japan.

[b.] Department of Materials Science and Engineering, Osaka Prefecture University, 1–1 Gakuen-cho, Naka, Sakai, Osaka 599–8531, Japan.

[c.] Trans-Regional Corporation Center for Industrial Materials Research, IMR, Tohoku University, 1–1 Gakuen-cho, Naka, Sakai, Osaka 599–8531, Japan.

*Correspondence Authors
E-mail: kezuka_yuki@shiraishi.co.jp
hmurata@mtr.osakafu-u.ac.jp

**This PDF file includes the following:**

## Supplementary Methods

### Characterization

**Brunauer–Emmett–Teller specific surface area (BET-SSA).** The BET-SSA of the prepared powders was measured *via* nitrogen adsorption[1,2] at 77 K using the Macsorb HM Model-1208 system (Mountech Co. Ltd., Japan). The samples were initially dried at 105°C for 1 h under vacuum before measurements.

**Inductively coupled plasma-atomic emission spectroscopy (ICP-AES) (alkaline–acid digestion).** For samples after heat treatment, which contain both $CaCO_3$ and $SiO_2$, the sample solutions were prepared according to the following steps: the sample powder (0.2 g) and fusion agent $Li_2B_4O_7$ (2 g) were placed in an open platinum pan and fused by heating in air for 1 h using a gas burner. The resulted melt was cooled down, dissolved with hydrochloric acid (~35%, 10 mL) and hot water, and agitated. The solution was then poured into a volumetric flask. 20 mL of yttrium solution (100 μg/mL) was added. The solution was diluted up to 200 mL with distilled water. No undissolved residues were observed. Si concentrations were measured *via* ICP-AES with an iCAP-6300 (Thermo Fisher Scientific Inc., USA). To obtain a calibration curve, a silicon standard solution (SPEX CertiPrep Inc., USA) was used.

**Table S1.** Si concentration conversion table

| Si concentrations versus $CaCO_3$ (ppm) | Si concentrations versus water (ppm) | Si/(Si+Ca) atomic ratio (-) |
|---|---|---|
| 460 | 68 | 0.0017 |
| 1900 | 270 | 0.0066 |
| 7800 | 1100 | 0.027 |
| 31000 | 4500 | 0.099 |

**Table S2.** BET-SSA and lattice parameters *a* and *c* of the nanoparticles as-synthesized and after slurry incubation

| | Si-coexisting amount | BET-SSA | lattice parameter | |
|---|---|---|---|---|
| | (ppm) | ($m^2/g$) | *a* (Å) | *c* (Å) |
| after slurry incubation | pristine | 12.4 | 4.9910 | 17.062 |
| | 460 | 13.5 | 4.9911 | 17.062 |
| | 1900 | 14.9 | 4.9912 | 17.061 |
| | 7800 | 19.1 | 4.9913 | 17.060 |
| | 31000 | 20.2 | 4.9914 | 17.059 |
| as-synthesized | pristine | 35.6 | 4.9920 | 17.057 |

BET-SSA of all the samples after the slurry incubation were smaller than the as-synthesized one, indicating that calcite growth had occurred during the slurry incubation. The decrease in BET-SSA became smaller with the increased concentration of Si. The degree of crystal growth was deduced to be suppressed by the coexistence of Si impurities. However, the amount of residual Si impurities may have also influenced the changes in BET-SSA values.

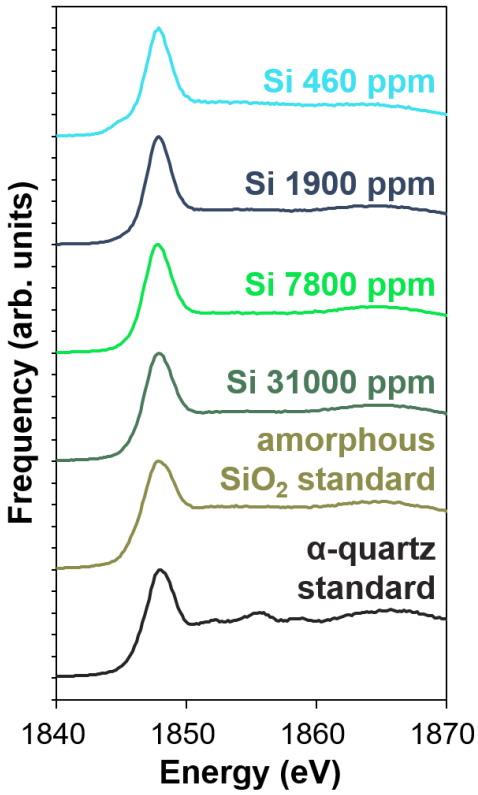


**Fig. S1.** Experimental Si-*K* X-ray adsorption near-edge structure (XANES) spectra of Si (460 ppm)-, (1900 ppn), (7800 ppm)- and (31000 ppm)-doped samples, amorphous silica and α-quartz standards.

The spectra of the Si-coexisted samples showed peak characteristics similar to one another and those of the amorphous $SiO_2$ standard. No peaks were observed in the post-edge region, which would have been observed in the presence of calcium silicates.[3] Combining these results with transmission electron microscopy (TEM) analyses, the irregular-shaped particles were determined to be amorphous $SiO_2$.

**Table S3.** Si concentrations, determined by ICP-AES, of the resulted powder samples after heat treatment with several different Si-coexisting amounts. The sample solutions were prepared by alkaline–acid digestion.

| Si-coexisting amount (ppm) | pristine | 460 | 1900 | 7800 | 31000 |
|---|---|---|---|---|---|
| detected Si content (ppm) | 10 | 450 | 1900 | 6700 | 28000 |

For the Si (460 ppm)- and (1900 ppm)-coexisted samples, almost 100% of Si added in the slurry existed in the powder by the solid-liquid separation method employed in this study. On the other hand, for the Si (7800 ppm)- and (31000 ppm)-coexisted samples, approximately 90% of Si added in the slurry existed in the powder, whereas the remaining amount of additives was considered to be separated during the filtration and washing process.

**Table S4.** Concentrations of impurity elements, determined by ICP-AES, in the pristine calcite particles before and after the slurry incubation at 95°C for 6 h in a beaker made of heat-resistant glass (borosilicate glass) instead of the Teflon beakers. The sample solution was prepared by acid digestion.

| | Si | B | Na | Al |
|---|---|---|---|---|
| before incubation (ppm) | 33 | 0.6 | 45 | 3.4 |
| after incubation (ppm) | 730 | 49 | 94 | 24 |

Increase in concentrations of borosilicate glass components (Si, B, Na, and Al) were detected, confirming the dissolution of the glass beaker during the incubation under high temperature/high pH conditions.

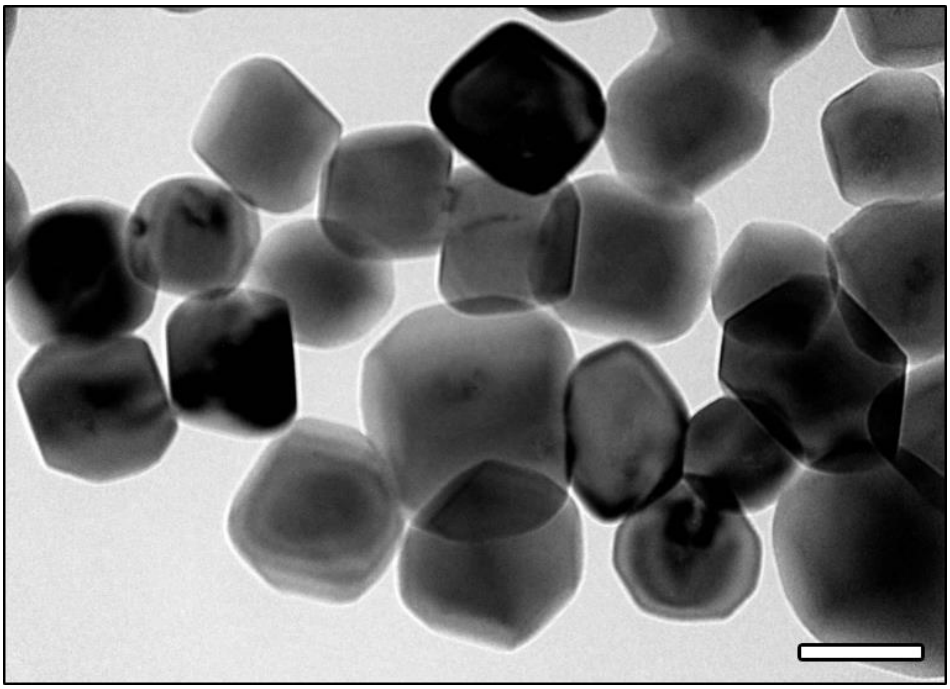

**Fig. S2.** The bright-field (BF)-TEM image of the pristine calcite nanoparticles after heat treatment (95°C for 6 h) in a beaker made of heat-resistant glass (borosilicate glass) instead of in a Teflon one. The scale bar is 100 nm.

Rhombohedral particles were observed. The resultant powder was found to contain Si 730 ppm by ICP-AES. Crystallite size and BET-SSA of this sample (99 nm and 14.4 $m^2/g$) were smaller and larger, respectively, than those of pristine (114 nm and 12.4 $m^2/g$) and even Si 460 ppm-coexisted (105 nm and 13.5 $m^2/g$) cases of the present study. The slight dissolution of glass beaker under high temperatures/high pH was found to significantly suppress the calcite growth due to the pH buffering effect proposed in this study. On the other hand, crystallite size and BET-SSA of this sample were larger and smaller, respectively, than those of Si 1900 ppm-coexisted case (97 nm and 14.9 $m^2/g$).

**Table S5.** Concentrations, in ppm, of various impurities in the starting material ($Ca(OH)_2$) determined by ICP-AES. The sample solution was prepared by acid digestion. Other impurity elements not listed here were under the detection limits.

| Si | Al | Cr | Cu | Fe | Li | Mg | Na | S | Sr | Zn |
|---|---|---|---|---|---|---|---|---|---|---|
| 9.2 | 3.8 | 1.8 | 0.5 | 5.6 | 2.8 | 4.6 | 57 | 18 | 1.2 | 1.4 |

The starting material ($Ca(OH)_2$) used in this study was confirmed to be of high-purity (4N grade).

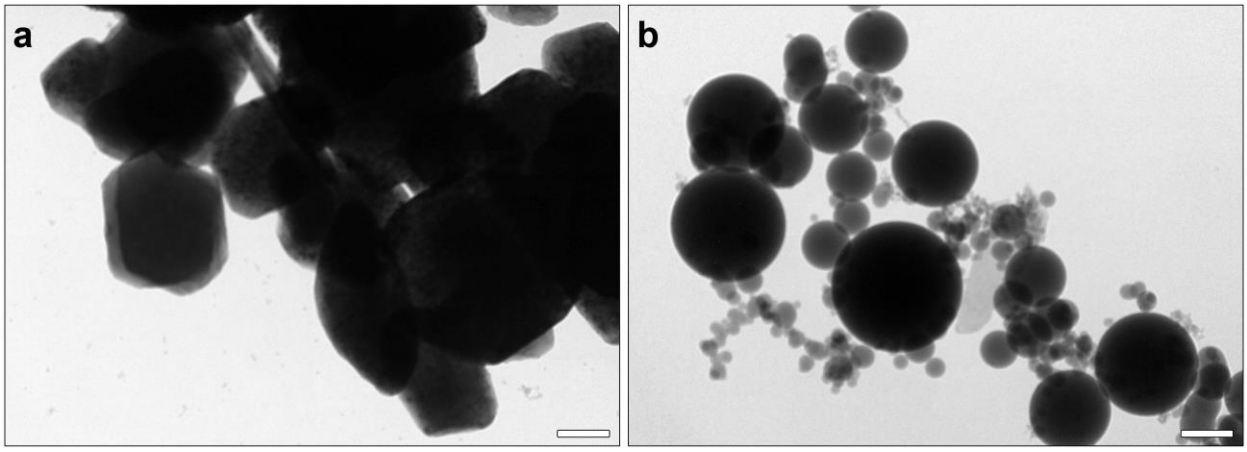


**Fig. S3.** The BF-TEM image of the (a) $Ca(OH)_2$ particles and (b) $SiO_2$ particles used as a starting material in this study. The scale bar is 200 nm.

BET-SSAs of the $Ca(OH)_2$ and reagent $SiO_2$ were measured to be 3.9 $m^2/g$ and 4.5 $m^2/g$, which corresponds to approximate spherical particle sizes of 700 nm and 610 nm, respectively.

## References


1 S. Brunauer, P. H. Emmett and E. Teller, The use of low temperature van der Waals adsorption isotherms in determining the surface area of iron synthetic ammonia catalysts, *J. Am. Chem. Soc.*, 1938, **60**, 309–317.

2 R. S. Mikhail and S. Brunauer, Surface area measurements by nitrogen and argon adsorption, *J. Colloid Interface Sci.*, 1975, **52**, 572–577.

3 J. Li, W. Zhang, K. Garbev and P. J. M. Monteiro, *Cem. Concr. Res.*, 2021, **143**, 106376.